AD-A161 821 VOID INITIATION PRECEDING DUCTILE FRACTURE IN POLYCRYSTALLINE TITANIUM..(U) VIRGINIA UNIV CHARLOTTESVILLE SCHOOL OF ENGINEERING AND APPLI.. 1/1

UNCLASSIFIED H G WILSDORF ET AL. SEP 85 F/G 11/6 NL

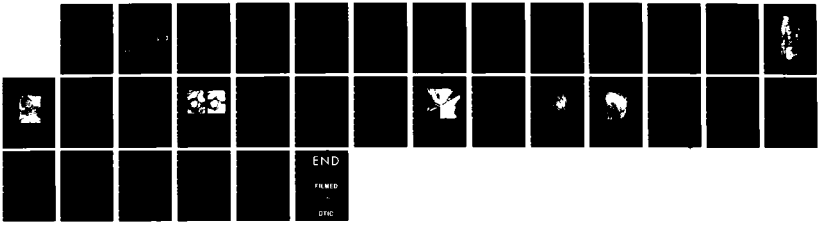

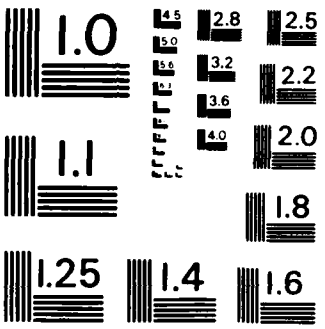

(12)

Technical Report

Contract No. N00014-82-K-0309-P00004

VOID INITIATION PRECEDING DUCTILE FRACTURE IN POLYCRYSTALLINE TITANIUM

Submitted to:

Office of Naval Research
800 North Quincy Street
Arlington, Virginia 22217-5000

Attention: Leader Materials Division, N00014
Associate Director for Engineering Sciences

Submitted by:

Heinz G. F. Wilsdorf
Professor

Marjorie A. Erickson
Research Assistant

Report No. UVA/525375/MS86/101

September 1985

SCHOOL OF ENGINEERING AND APPLIED SCIENCE

DEPARTMENT OF MATERIALS SCIENCE

UNIVERSITY OF VIRGINIA
CHARLOTTESVILLE, VIRGINIA 22901

Technical Report

Contract No. N00014-82-K-0309-P00004

VOID INITIATION PRECEDING DUCTILE FRACTURE IN POLYCRYSTALLINE TITANIUM

Submitted to:

Office of Naval Research
800 North Quincy Street
Arlington, Virginia 22217-5000

Attention: Leader, Materials Division, N00014
Associate Director for Engineering Sciences

Submitted by:

Heinz G. F. Wilsdorf
Professor

Marjorie A. Erickson
Research Assistant

Department of Materials Science
SCHOOL OF ENGINEERING AND APPLIED SCIENCE
UNIVERSITY OF VIRGINIA
CHARLOTTESVILLE, VIRGINIA

Report No. UVA/525375/MS86/101

Copy No. _____

September 1985

Unclassified
SECURITY CLASSIFICATION OF THIS PAGE (When Data Entered)

REPORT DOCUMENTATION PAGE		READ INSTRUCTIONS BEFORE COMPLETING FORM
1. REPORT NUMBER	2. GOVT ACCESSION NO. AD-A161 921	3. RECIPIENT'S CATALOG NUMBER
4. TITLE (and Subtitle) VOID INITIATION PRECEDING DUCTILE FRACTURE IN POLYCRYSTALLINE TITANIUM		5. TYPE OF REPORT & PERIOD COVERED Technical Report
		6. PERFORMING ORG. REPORT NUMBER UVA/525375/MS86/101
7. AUTHOR(s) Heinz G. F. Wilsdorf Marjorie A. Erickson		8. CONTRACT OR GRANT NUMBER(s) N00014-82-K-0309
9. PERFORMING ORGANIZATION NAME AND ADDRESS Department of Materials Science University of Virginia, Thornton Hall Charlottesville, VA 22901		10. PROGRAM ELEMENT, PROJECT, TASK AREA & WORK UNIT NUMBERS P00004
11. CONTROLLING OFFICE NAME AND ADDRESS Office of Naval Research 800 N. Quincy Street Arlington, VA 22217-5000		12. REPORT DATE September 1985 13. NUMBER OF PAGES
14. MONITORING AGENCY NAME & ADDRESS (if different from Controlling Office) ONR Resident Representative Joseph Henry Building, Room 623 2100 Pennsylvania Avenue, N.W. Washington, DC 20037		15. SECURITY CLASS. (of this report) Unclassified 15a. DECLASSIFICATION/DOWNGRADING SCHEDULE

16. DISTRIBUTION STATEMENT (of this Report)

Unlimited

17. DISTRIBUTION STATEMENT (of the abstract entered in Block 20, if different from Report)

18. SUPPLEMENTARY NOTES

19. KEY WORDS (Continue on reverse side if necessary and identify by block number)

Ductile fracture
Void initiation
Void growth
Stereo-photogrammetry

20. ABSTRACT (Continue on reverse side if necessary and identify by block number)

The objective of this research was determination of primary void initiation sites preceding void growth in the process of deformation leading to ductile fracture in polycrystalline C.P. titanium. Stereo-photogrammetry was employed to evaluate SEM fracture surfaces. Two distinct regimes of void initiation were found to operate in: (i) specimens with grain sizes up to 50 μm void initiation occurring predominately at grain boundary triple points; (ii) larger grain sized material. Here, additional void sites were due to

DD FORM 1 JAN 73 1473 EDITION OF 1 NOV 65 IS OBSOLETE

Unclassified
SECURITY CLASSIFICATION OF THIS PAGE (When Data Entered)

20. ABSTRACT (continued)

twinning and glide band intersections and to dislocation interactions with grain boundaries and grain boundary ledges themselves. Quantitative topographical information was the basis for constructing fracture surface profiles which permitted the determination of time sequence of void initiation.

TABLE OF CONTENTS

VOID INITIATION PRECEDING DUCTILE FRACTURE IN POLYCRYSTALLINE TITANIUM

Marjorie A. Erickson* and Heinz G. F. Wilsdorf
Department of Materials Science
University of Virginia
Charlottesville, Virginia 22901

1. INTRODUCTION

While void initiation has been covered in fair detail for particle containing alloys [1,2], experimental evidence in pure or relatively pure polycrystalline ductile metals has received only scant attention, except for fracture at higher temperatures [3]. Under creep conditions grain boundary sliding often leads to void formation at grain boundary triple points (GBTP) and theoretical models for the high temperature regime have been published [4,5]. One cannot expect that these mechanisms are operative in high melting point metals at room temperature, and plastic deformation has been invoked for void initiation by assuming the development of pile-ups when dislocations were unable to penetrate grain boundaries [6,7,8]. Also, grain boundary ledges have been thought to initiate microcracks [9]; other mechanisms are based on crossing slip bands [10], or intersecting twins [11], and bend planes [7,12].

The present investigation has as its objective to determine the locations of primary void initiation sites. Fracture experiments were made with C.P. titanium under tensile loading, and fracture surfaces were examined with a scanning electron microscope (SEM). The crack path in most metals is a tortuous one, and this is particularly true for titanium. It was found necessary to employ stereo-photogrammetry in order to obtain true measurements of fracture surface features.

2. SAMPLE PREPARATION AND EXPERIMENTAL PROCEDURE

Tensile samples were prepared from a 0.198 cm thick sheet of C.P. titanium. The material was 99.838% pure with an impurity content that included O, N_2, C, H_2 and Fe_2. After polishing the gauge sections of each sample with grit size decreasing to 600 grit and heat treating, the gauge

---

*Current Address: David W. Taylor Naval Ship R&D Center, Annapolis Laboratory, Annapolis, Maryland 21402-5067.

lengths and cross-section areas of each sample were carefully measured. Once fracture occurred pieces containing the fracture surfaces were carefully cut approximately 0.5 cm from the fracture edge and mounted onto an aluminum specimen stub for subsequent SEM study.

A range of heat treatments was done to vary the grain size of samples to allow a study of grain size versus tensile properties and fracture surface characteristics. Because of sample purity only the α-phase of Ti is present at room temperature, so stress relief, recrystallization and grain control were the primary goals of heat treating.

Ten samples were prepared for study. Heat treatments were designed to cause a variation in grain size from 13 μm to 1300 μm. Table 1 lists the various samples with the heat treatment they were given and their resulting grain size.

To prevent oxygen from diffusing into the samples during heat treating, each sample was enclosed in a quartz tube evacuated to 5×10^{-7} torr.

For grain size determination, a piece from the shoulder of each sample was cut, mounted onto an SEM stub, encased in epoxy, and polished and etched in a solution of 10 ml HF, 5 ml HNO_3 and 85 ml distilled water for $1\frac{1}{2}$ minutes.

The tensile specimens were pulled to fracture on an Instron Universal Testing Machine. The crosshead speed was either 0.05 cm/sec or 0.005 cm/sec. Load vs. time was recorded and from this tensile properties were determined.

Fractographs of the entire surface were taken of opposing surfaces at low magnifications, using stereo techniques, as references for future higher magnification micrographs. These low magnification fractographs were also used to measure final cross-sectional area at the fracture to determine the reduction in area of each sample.

A number of pictures were taken at higher magnifications (300x to 1000x), using stereo techniques to enable a detailed three-dimensional study of the fracture surface. Thus, fracture surface features could be determined accurately by making measurements of relative height as well as relative horizontal distances.

Studies of microstructures were related to studies of fracture surface features to pinpoint primary void initiation sites in α-Ti. Five to ten micrographs of each sample, polished and etched for grain size measurements, were enlarged and used to determine grain size using the grain boundary-line intercept method. These pictures were also used to measure intertriple point

TABLE I

GRAIN SIZES OF FRACTURE SPECIMENS

SAMPLE	HEAT TREATMENT	Average Grain Size	Range
1	½ hr. at 700°C furnace cool	13 μm	1-55 μm
2	½ hr. at 700°C air cool	21 μm	2-72 μm
3	2 hrs. at 700°C air cool	46 μm	7-188 μm
4A	2 hrs. at 1000°C air cool	178 μm	30-1210 μm
4B	2 hrs. at 1000°C air cool	200 μm	27-1215 μm
5A	5 hrs. at 1175°C furnace cool	427 μm	40-1550 μm
5B	5 hrs. at 1150°C furnace cool	420 μm	35-1490 μm
6	8½ hr. at 1150°C furnace cool	792 μm	70-1880 μm
7A	20 hrs. at 1150°C furnace cool	1247μm	82-2150 μm
7B	20 hrs. at 1150°C furnace cool	1310μm	79-2120 μm

distances by direct measurements. Measurements were made over areas of ~1000 μm^2 for small grained samples and 1000^2 - 2000^2 μm^2 for larger grained samples.

Measurements of dimple diameter and inter-dimple distances were taken directly from stereo micrographs which allowed evaluations in 3-dimensions. Dimple diameters were taken as the line through the center of the dimple perpendicular to the long axis of the dimple. Interdimple distances were measured from the center of one dimple to the center of an adjacent dimple taking relative height variations into account by making measurements using a Hilger-Watts stereo viewer.

3. RESULTS

Significant mechanical properties of typical tensile samples are listed in Table 2.

An evaluation of measurements obtained from SEM fractographs indicated immediately that in small grain specimens interdimple distances corresponded primarily to intertriple point distances. This can be clearly seen in Fig. 1; the measurements were taken from specimens 1-3 with average grain sizes of 13 μm, 21 μm, and 46 μm, respectively. The fit of the second peak of interdimple spacings with intertriple point spacing peaks is amazingly good. Notably, there is on each of these graphs a higher peak for interdimple spacings which lies between 1 μm and 3 μm. The significance of this maximum peak will be discussed in the following section. Figure 2 gives an impression of dimple size distributions in a fracture surface of specimens having grain sizes below 50 μm.

The character of fractographs changed drastically for specimens with grain sizes of 200 μm and larger (Fig. 3). Instead of only a broad distribution of dimple sizes over the whole fracture surface, elongated ridges are also seen over a relatively large area. Dimple size distributions for four grain sizes are given in Fig. 4. For these samples, interdimple distances and intertriple point distances are unrelated although the maximum peak of the first group is retained at 1 μm to 3 μm. The change in the fracture surface characteristics between specimens with "small" and "large" grains indicates the presence of two distinct mechanisms of void initiation.

TABLE II

TENSILE PROPERTIES FOR FOUR SAMPLES WITH DIFFERENT GRAIN SIZES

Sample	Grain Size (μm)	Engineering Y.S. ($\times 10^8$ Pa)	Engineering U.T.S. ($\times 10^8$ Pa)	Engineering F.S. ($\times 10^8$ Pa)	True Y.S. ($\times 10^8$ Pa)	n	%El.	RA
1	13	3.68	4.37	3.19	3.76	0.169	17.7	59.4%
2	21	3.87	4.62	3.24	3.91	0.120	22.9	64%
3	46	3.45	4.18	2.96	3.49	0.128	19.9	64.1%
5A	427	2.50	2.98	0.72	2.53	0.152	18.7	64.4%

El. = Elongation to fracture; RA = Reduction in area

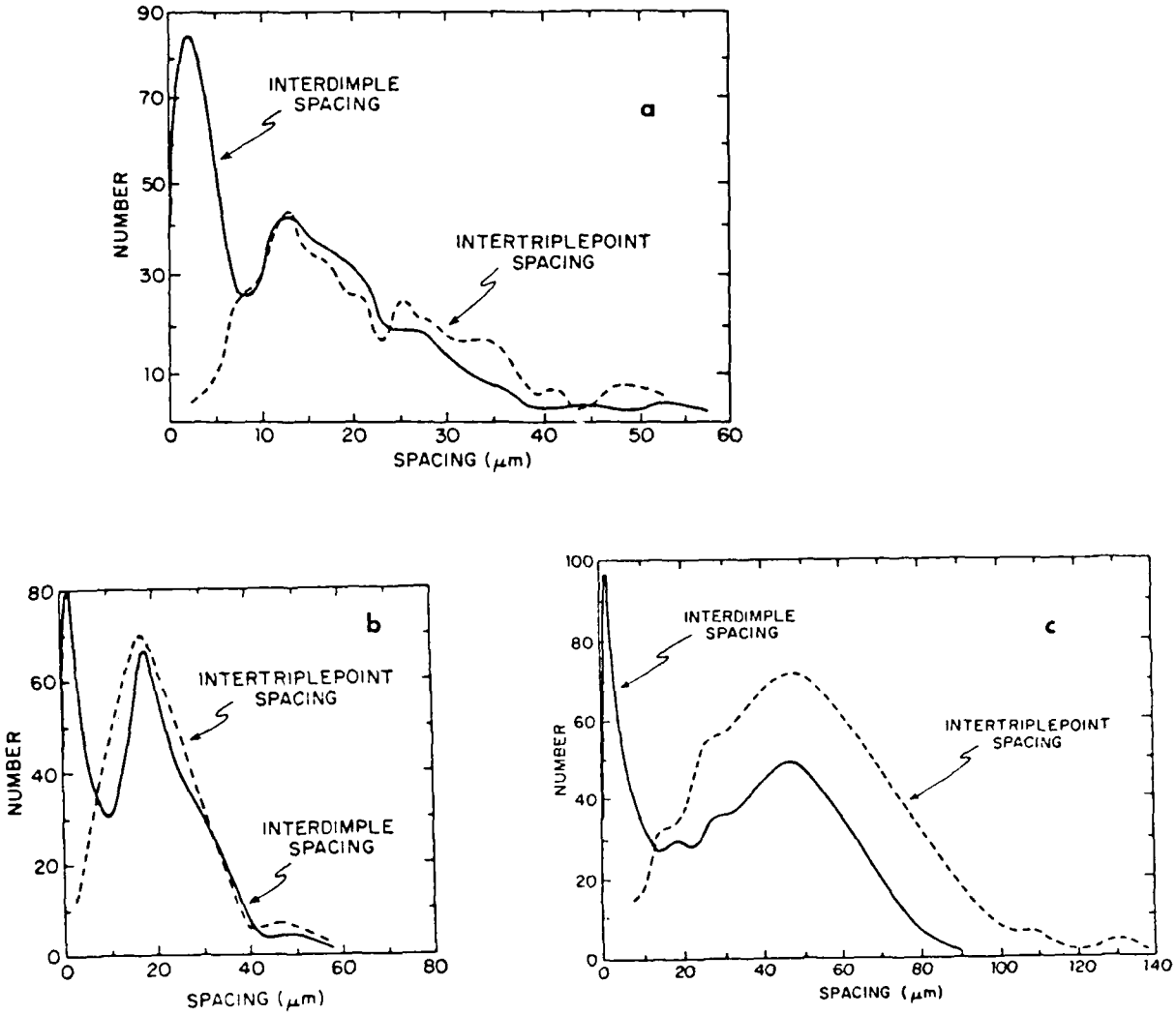

Fig. 1. Comparison between the numbers of interdimple and intertriple point spacings for specimens with average grain sizes of 13, 21 and 46 μm corresponding to specimen numbers 1, 2, and 3.

Fig. 2. SEM fractograph of specimen #2 having an average grain size of 21 µm. Range of grain sizes from 2 to 72 µm. The bottom levels of dimples A, C and B are at 10 µm, 5 µm and 0 base, respectively, as determined by stereo-photogrammetry. The ridge on the right of dimple B (arrow) is almost 40 µm higher than the bottom level of B.

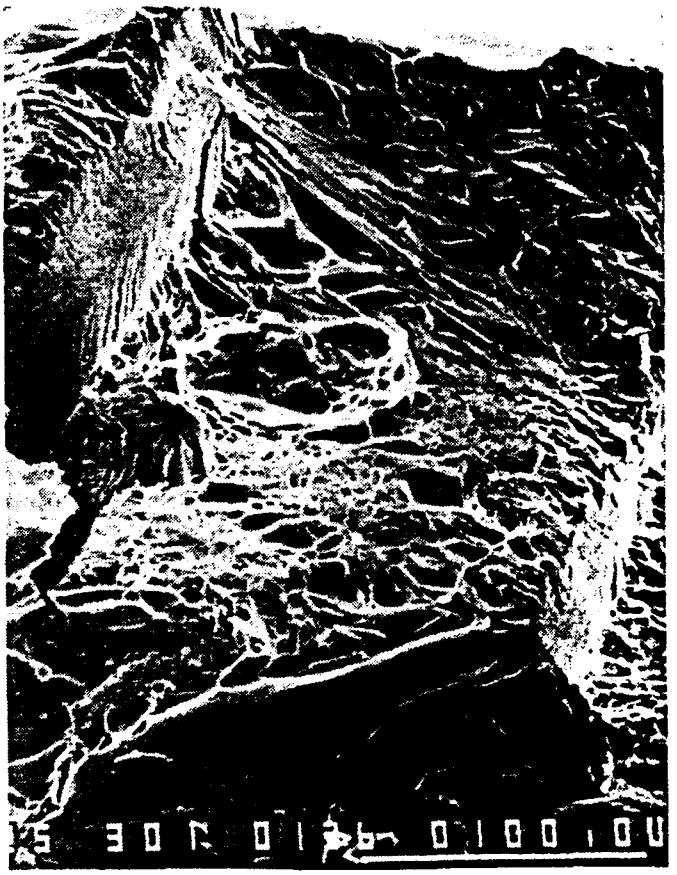

Fig. 3. SEM fractograph of specimen #7A with average grain size of 1,250 μm. Note numerous dimples in the center area and grain boundary ledges at lower right. Range of grain sizes: 82 μm to 2,150 μm.

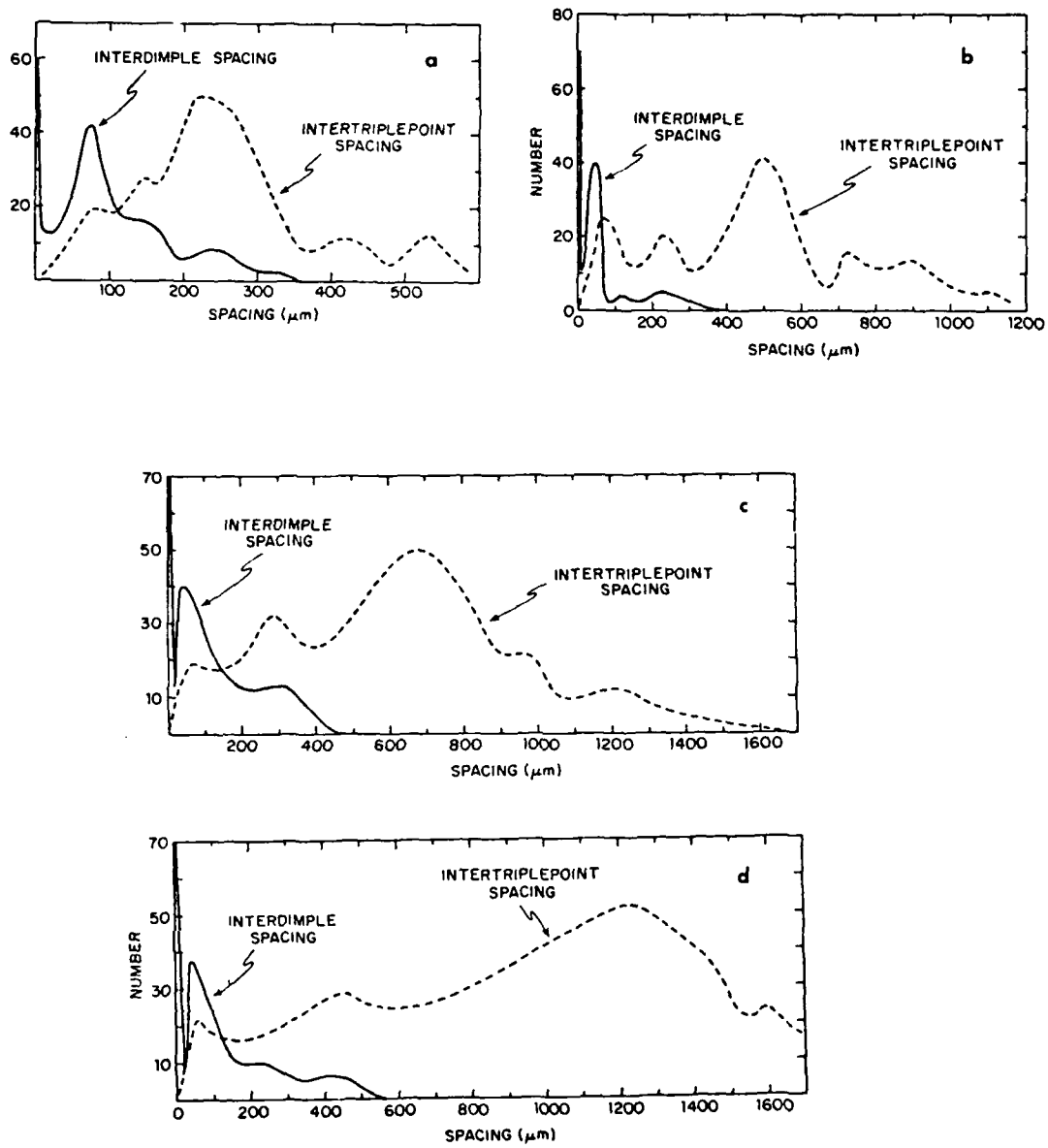

Fig. 4. Comparison of frequency of interdimple and intertriple point spacings for four large grained specimens. Average grain sizes were 200, 427, 792, and 1,250 μm corresponding to specimens 4B, 5A, 6 and 7A, respectively.

The measurements displayed in Fig. 1 and 4 were made from stereo-pairs. A simple addition to a flying spot stereo-microscope made it possible to draw topographical maps of fracture surfaces. An example is given for a rather simple fractograph, Fig. 5, for which a stereo-pair is shown. The corresponding topographical map is given in Fig. 6. While stereo-viewing conveys a distinct three-dimensional impression of the general layout of a fracture surface and also of individual dimple geometries, it would not have been possible to conceive the large difference between the lowest points of the dimples. The largest height difference measured in this micrograph amounts to 40.8 μm. Dimple #1 has an average depth of 24 μm while dimples #2 and #3 have average depths of 13 μm and 10 μm, respectively. The stereo-photogrammetry revealed not only that the dimple depths are different by larger amounts than what the eye had perceived but that the base surface is inclined, i.e., it increases from top right of Fig. 5 to bottom left. The even greater complexity of the topography in large-grained specimens is now appreciated and stereo pairs are essential for their evaluation.

For a complete evaluation of fracture surfaces, however, one has to go one step further. From the irregular features seen in all stereo-micrographs, one must draw the conclusion that the growth of voids depends on local stress conditions at a microstructural scale and consequently is anisotropic. Therefore, one can expect that matching fracture surfaces will look differently, and the drawing of contour maps has shown this convincingly. Figure 7a depicts a cut through contour maps of matching fracture surfaces. In order to classify the difference in the features of these matching surfaces, the vertical scale has been enlarged by a factor of five. The true profile for the "lower" surface is shown in Fig. 7b.

4. DISCUSSION

The immediate problem is to rationalize the effects of grain boundary structures on void initiation. The dimple measurements show that there are two relationships between interdimple distances and intertriple point distances: one group with grain sizes below 50 μm has an almost perfect correspondence between these data points, while for another group with grain sizes above 200 μm this relationship is not the dominating one.

Crack initiation at triple points is common in creep as first explored by Zener [13]; here grain boundary glide was involved and thereby a triple point

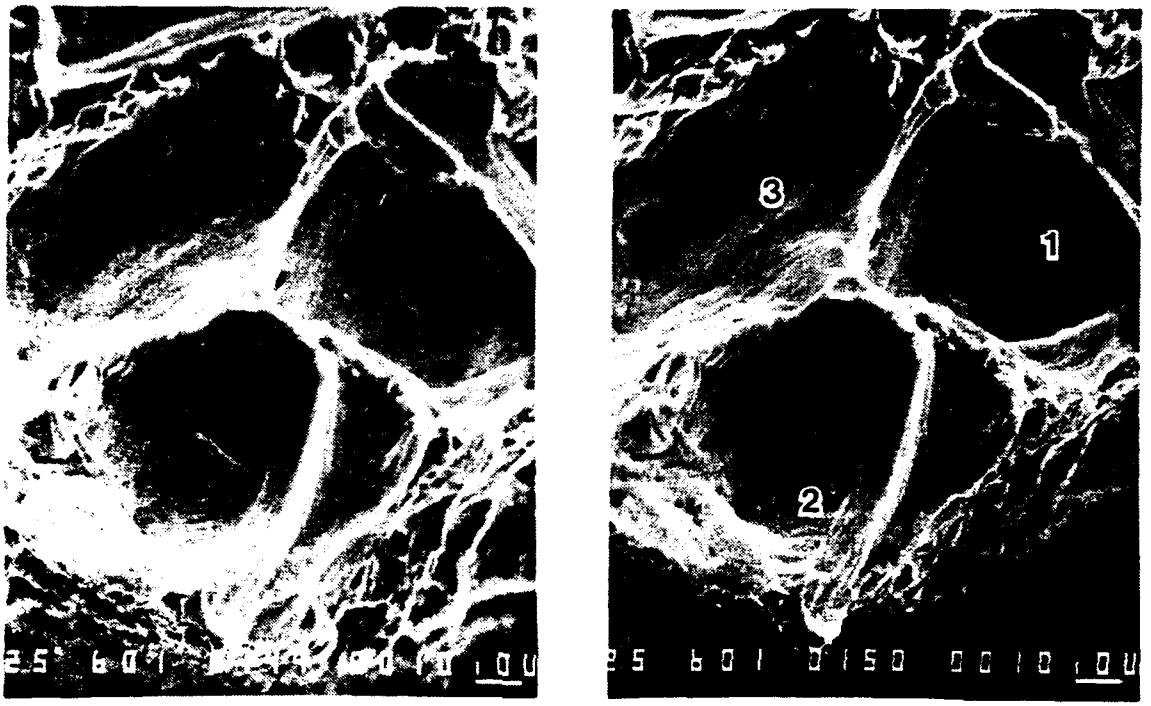

Fig. 5. Stereo-pair of dimples in specimen #3 with average grain size of 46 μm.

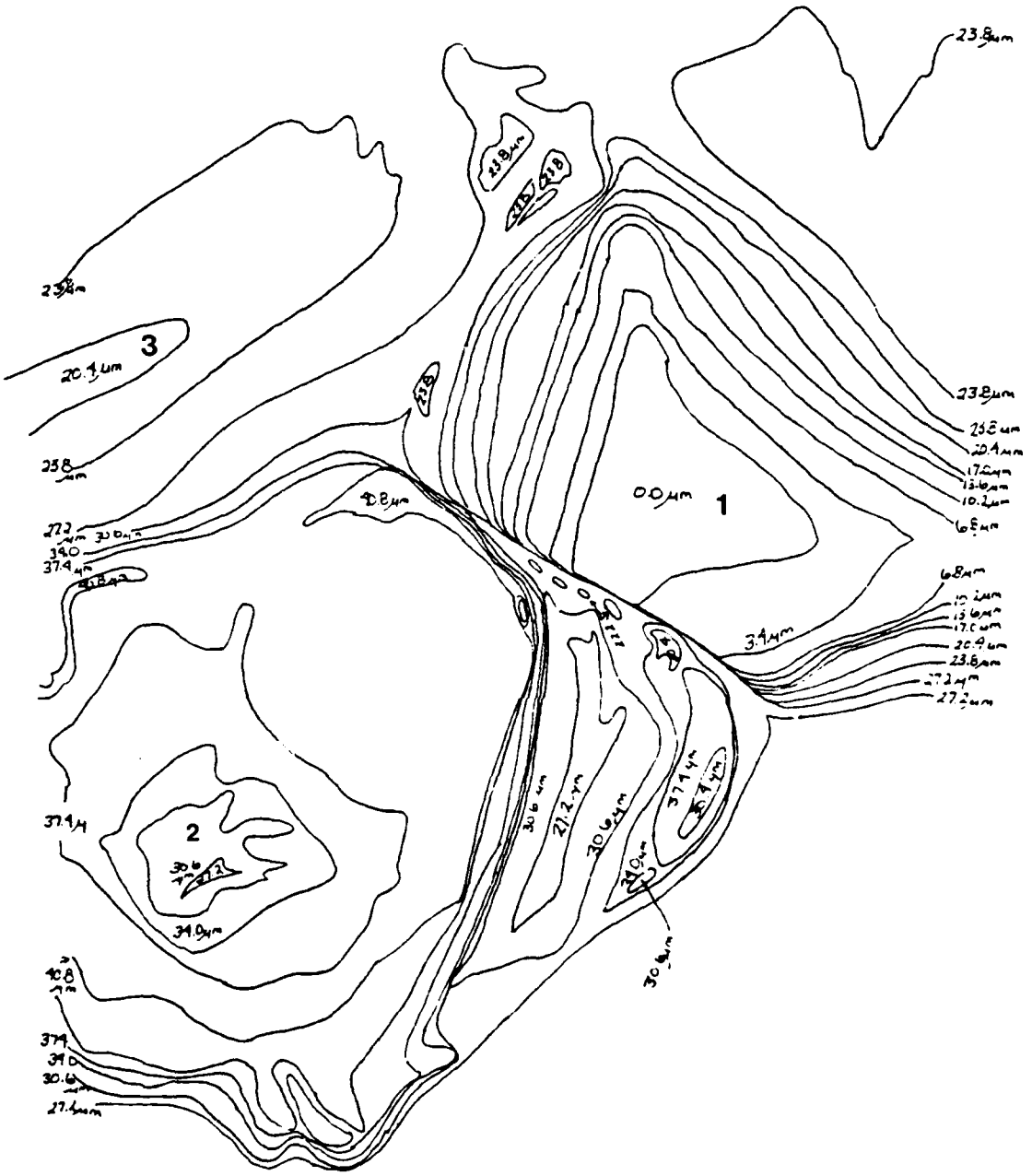

Fig. 6. Topographical map constructed from stereo-pair shown in Fig. 5. For details of mapping see M.S. Thesis of Marjorie A. Erickson, Univ. of Virginia, 1983.

7(a).

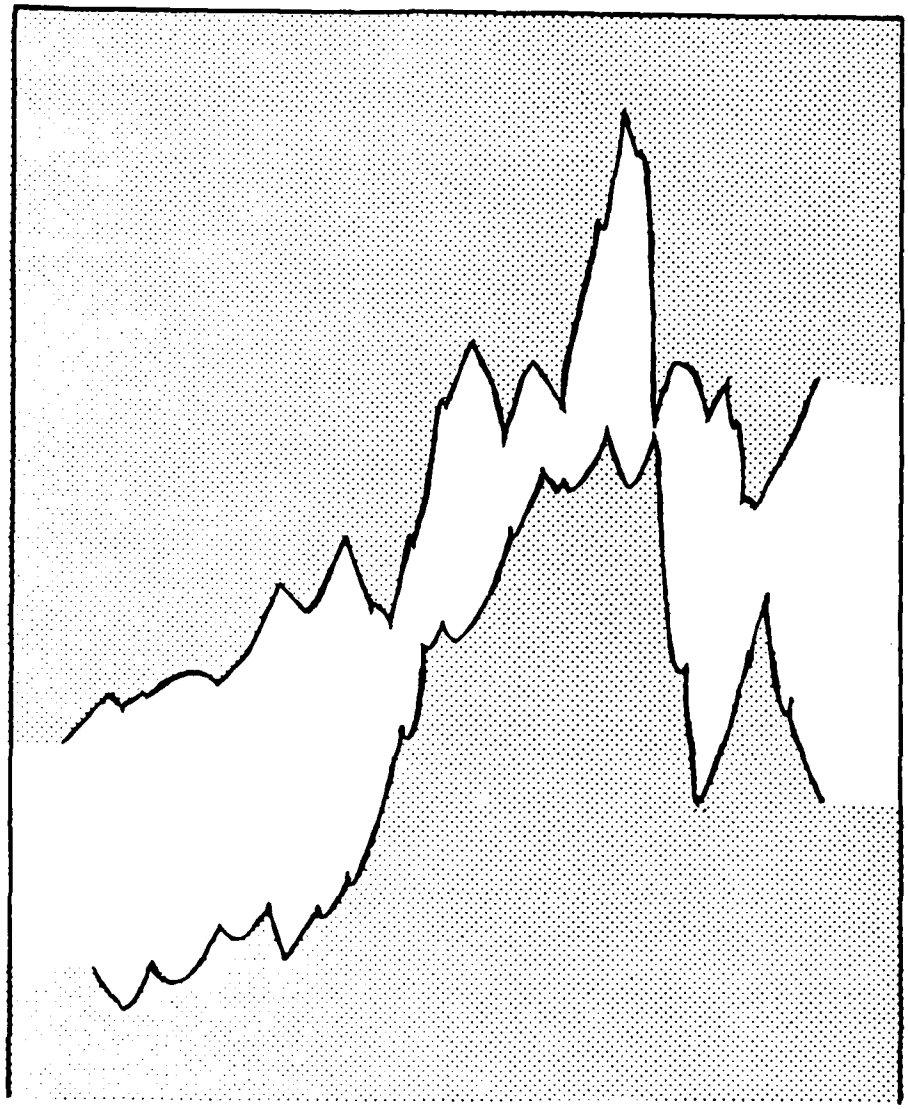

7(b).

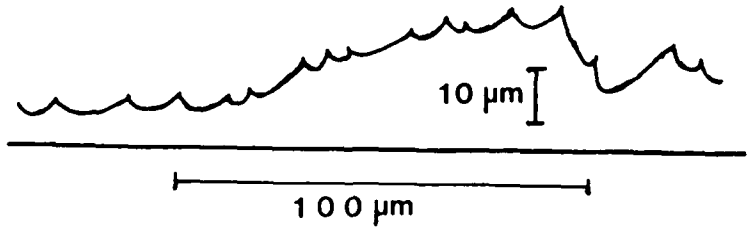

Fig. 7(a) Upper and lower profiles of a cross-section of a fracture surface taken by SEM from specimen #3. Note differences between the two profiles. Clearly, a characterization of fracture surfaces requires stereo-photogrammetry of corresponding fractographs. Vertical axis magnified by a factor of five. See lower profile at 7(b) for normal scale.

becomes the obvious location for a stress concentration. Movement between grains along their boundary is not to be expected in titanium at room temperature. However, incompatibility stresses between grains [14] should be high at triple points. In-situ straining in a TEM showed that the first glide dislocations are often generated at triple points (see Fig. 8 [15]), and slip lines have been seen to originate at triple points [16]. Recently Kurzydlowski et al. concluded on the basis of in-situ TEM work in stainless steel that the emission of dislocations from a triple point occurs at a stress of G/320, with G the shear modulus [17]. These authors claim that the stress concentration factor of a triple point is not far from 2.8 [17,18]. All of this indicates that after extensive deformation, a triple point represents an exceptionally high local stress concentration in a polycrystalline material. In addition, it is known that impurities reduce the energy in grain boundaries [19] and this most likely applied to our case. The experimental result that grain boundary triple points have been the primary sites for void initiation is thus understandable. The question now to be treated is concerned with the observation that for specimens with grains larger than 200 μm this does not hold.

Since the reduction in area for all specimens was 60% or higher, the plastic deformation in the neck was substantial. Titanium deforms at room temperature by prism glide, $\{10\bar{1}0\}\langle 11\bar{2}0\rangle$, and by twinning on six planes [20]; the most frequently observed twins have $\{10\bar{1}2\}$ and $\{11\bar{2}2\}$ as composition planes. The influence of twinning on void initiation has to be included in our deliberations since it is well known that twinning plays an important role in larger grained titanium while deformation twins have not been seen in small grained titanium [21]. Mechanical twinning will occur in Ti for $\{10\bar{1}2\}\langle 10\bar{1}1\rangle$, for example, by stresses in tension parallel to the c-axis and correspondingly for compression stresses perpendicular to it. That both types of stresses can act at grain boundaries cannot be doubted since after even modest strains, grain boundaries will have developed ledges, the stress fields of which have been calculated by Das and Marcinkowski [9]. Amateau et al. reported the occurrence of twins in α-Ti (O_2 = 0.25% as compared to our O_2 = 0.102%) after a strain of 4.8% for specimens with grain sizes comparable to our specimen #4 [22]. These authors identified "thick" twins as $\{10\bar{1}2\}$ and

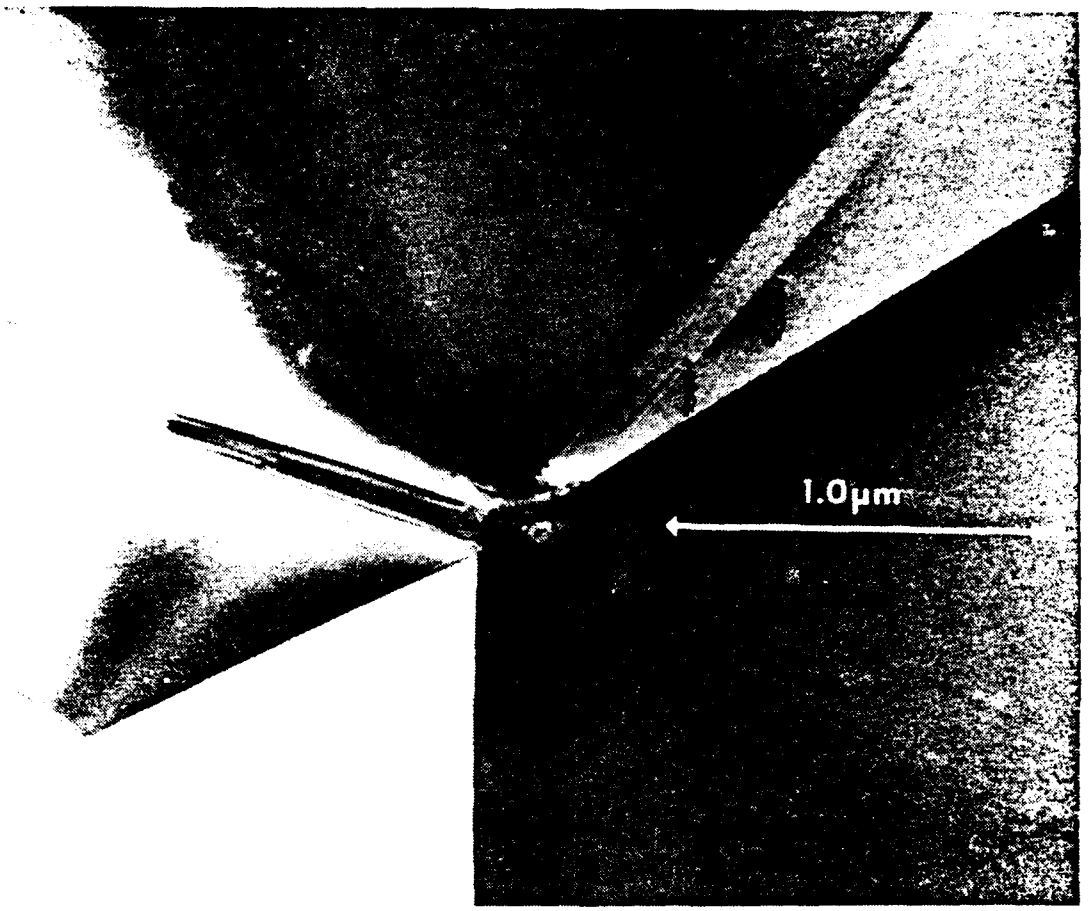

Fig. 8. Initiation of first dislocations at triple point area upon straining at 304 stainless steel foil. In-situ TEM experiment.

$\{11\bar{2}2\}$ types and "thin" twins of $\{11\bar{2}x\}$ types with x = 1, 3, or 4 (second order twins) in accordance with the findings of Rosi et al. [23]. The second order twins were seen in the $\{11\bar{2}2\}$ twins and the crack nucleation occurred between second order twins and matrix based on observations by light microscopy at 180°K. Figure 9 shows a fracture surface in support of this mechanism. In stereo-viewing one can see a fine ridge structure with a spacing of a few micrometers lying within larger bands 10 μm to 30 μm wide. The latter fit the description of the "thick" $\{11\bar{2}2\}$ twins and the finer lamellae the secondary twins. A grain boundary is indicated by arrows. Intergranular fracture obviously has produced the relatively flat area marked A. Arrows B are pointing to two deep microcracks. While Fig. 9 represents an extreme case of crack initiation by twinning processes, Fig. 10 is indicative of slip and twinning which are both present in areas about a few hundred micrometers across where void initiation by glide and initiation of microcracks by twinning operated in close proximity in grains between 200 and 1,300 μm.

In Fig. 11 we have plotted the maxima of interdimple spacings against grain size and one can see that the interdimple spacing follows the grain size for the grains and then levels off regardless of grain size. All measurements of interdimple spacings have been made from only those areas of fracture surfaces which showed full ductility. As seen from Fig. 4, the broad distribution of dimples is not uniform but shows in addition to the maximum of about 50 μm a number of smaller peaks. The same is true for the intertriple point spacing with its maximum near the average grain size. It should be noted that for the four grain sizes (Fig. 4) a small peak of intertriple point spacings coincides with a peak of interdimple spacings. Again the indication is that triple points remain important void initiation sites. However, other void initiation processes are now more competitive. Besides initiation sites at grain boundary ledges and secondary twin-matrix intersections, other processes must have been active. The "bend plane" mechanism is normally cited as an important crack nucleation model for hexagonal crystals but is not applicable for highly strained polycrystalline Ti since that mechanism is based on bicrystal studies in zinc at low temperatures where cracks appeared parallel to the basal plane after elongations to fracture of only 0.5% to 2.8% [12]. All of our samples showed multiple glide in the necked region which

Fig. 9. SEM fractograph indicative of primary and secondary twinning as a cause of fracture.

Fig. 10. SEM fractograph showing ridge structures due to twinning and/or glide. A reasonable smooth surface (i.e. without dimples) rises almost perpendicular and indicates a brittle component of the fracture process; this plane is indicated between arrows.

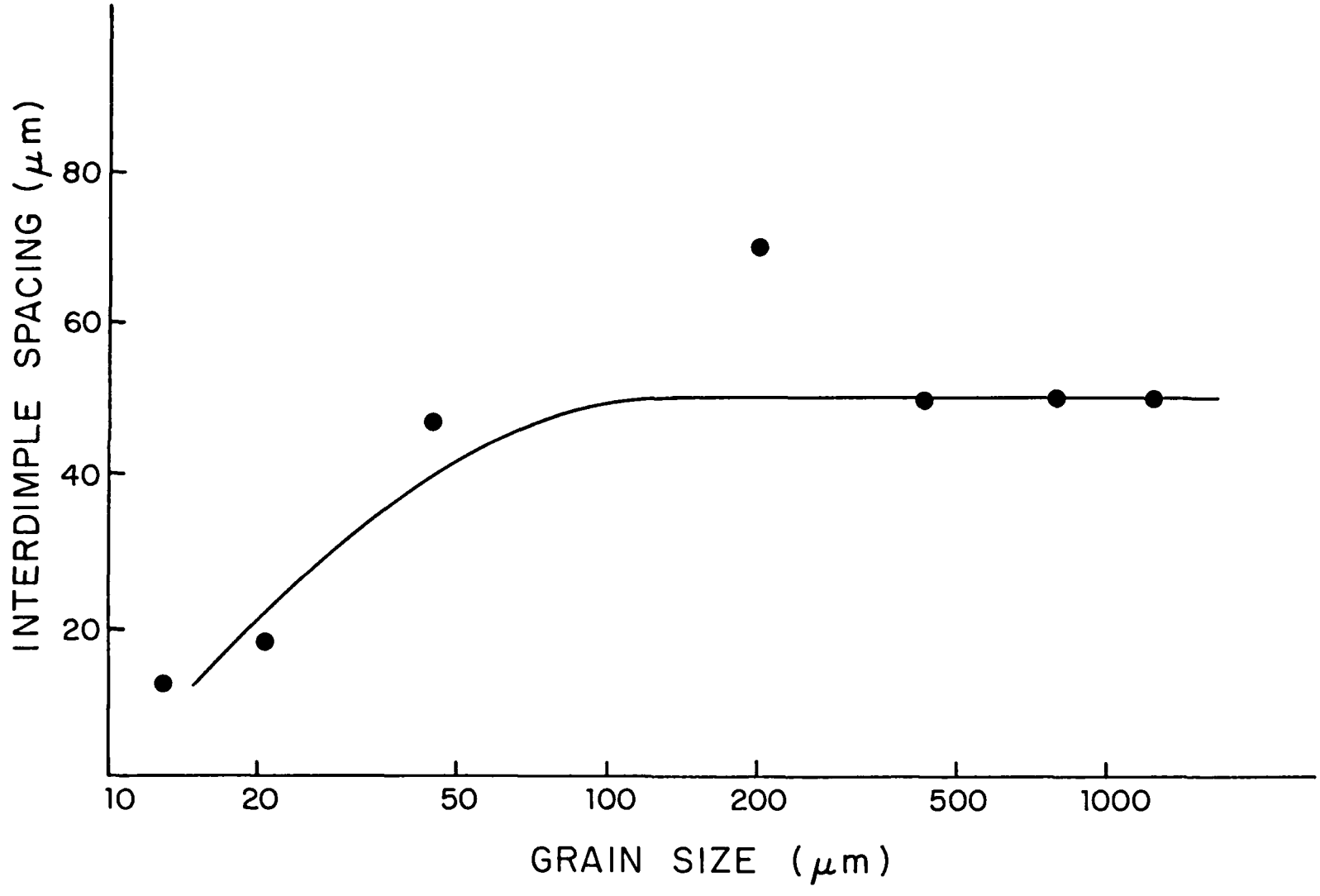

Fig. 11. Relationship between interdimple spacings and grain size.

means that extensive glide was produced by a number of glide systems crossing each other. Microcrack initiation at slip intersections in close packed crystals has been considered as one of the most important void initiation mechanisms [10], and it is proposed that this mechanism also participates in polycrystalline Ti. The significant peak for interdimple spacings in Fig. 4 is consistently at or near 50 μm in larger grain size material and gives credence to a glide crossing mechanism for prime void initiation sites for large-grained Ti.

Close inspection of SEM fractographs shows that the largest number of voids grows only to a diameter of about 1 μm as documented by the highest peaks for interdimple spacings in Figs. 1 and 3. Earlier work on the initiation of microcracks in heavily workhardened metals and alloys [25,26,27,28,29] pointed to the importance of dislocation cell walls for microvoid initiation. This is exactly the situation in the micro-ligaments between the large voids discussed so far. Here $\varepsilon>1$ on account of the continuous reduction in thickness of the micro-ligaments to a few micrometers. A detailed description of microvoid initiation and growth has been given elsewhere [30]. The microdimples under discussion are seen primarily on the rims of larger dimples and indicate areas where localized rupture has taken place.

A determination of the profile of a dimpled fracture surface can provide information as to the precise sequence of void initiation, provided the resolution of the technique is high enough to discern the relationships between dimples for the two opposite fracture surface profiles. The profiles in Fig. 7 have been evaluated for a time sequence by first "closing" the fracture, i.e., moving the upper and lower profiles over each other so that no white areas remain; then moving the profiles apart, one can monitor the initiation sequence (see Fig. 12 for the appearance of initiation of voids [1-3]). Measuring the whole sequence of 16 initiation sites yields an average distance between sites of nearly 10 μm. With an average grain size of 13 μm in this specimen the claim of triple points as primary initiation sites (see Fig. 1) is verified within the error limits. This determination was made under the assumption that void growth is proportional to time, and that the profile would be going through the center of the dimples which is, of course, not fulfilled. A more careful analysis would involve profiling at close intervals which, if done for a larger part of the fracture surface, would contribute to the quantitative topographical characterization of the time

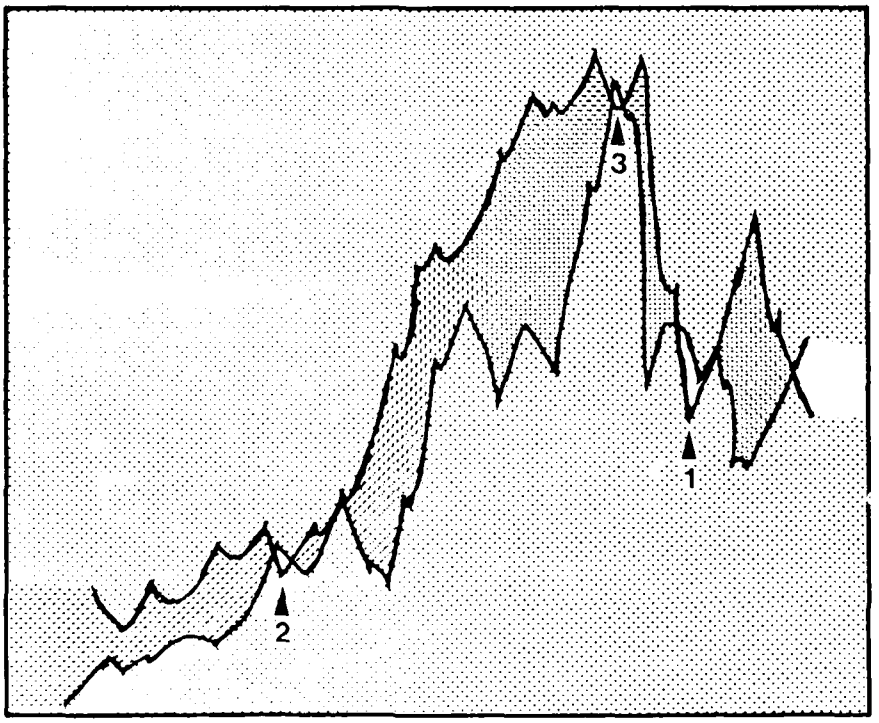

Fig. 12. Use of fracture surface profiles for determining void initiation time sequence. Vertical axis magnified by a factor of five for clarity.

sequence of void initiation. This measurement is adding the dimension of time to the study of voids in fracture surfaces at microscopic resolution for the first time.

5. CONCLUSIONS

(a) In specimens up to grain sizes of 50 μm, grain boundary triple points are primary void initiation sites.

(b) When grain sizes range between 200 μm and 1,300 μm additional void initiation sites are provided by twin intersections, glide band intersections, dislocation interactions with grain boundaries, and grain boundary ledges.

(c) Microvoids are seen at the rims of dimples and between dimples; they are due to initiation at dislocation cell walls and occur during rupture at the final separation.

(d) The time sequence of void initiation can be derived from fracture surface profiles which were constructed from quantitative topographical information.

(e) It has been demonstrated that quantitative stereo-photogrammetry for the characterization of fracture surfaces is mandatory.

REFERENCES

1. D. Brock, Eng. Fract. Mech. 5 (1973) 55.

2. J.D. Boyd and R.G. Hoagland, in Titanium Science and Technology, Plenum Press, NY (1973) pp. 1071.

3. J.N. Greenwood, D.R. Miller and J.W. Suiter, Acta Metall. 2 (1954) 250.

4. R.D. Gifkins, Acta Metall. 4 (1956) 98.

5. H.C. Chang and N.J. Grant, Trans. Met. AIME 206 (1956) 545.

6. C. Zener, in Fracturing of Metals, ASM, Metals Park, Ohio, 1948, p. 3.

7. A.N. Stroh, Phil. Mag. 3 (1958) 597.

8. J.J. Gilman, Trans AIME 212 (1958) 783.

9. E.S.P. Das and M.J. Marcinkowski, J. Appl. Phys. 45 (1972) 4425.

10. A.S. Argon and E. Orowan, Nature 192 (1961) 447.

11. D. Hull, in Fracture of Solids, Wiley, NY, 1963, p. 417.

12. J.J. Gilman, Trans AIME 200 (1954) 621.

13. C. Zener, Elasticity and Anelasticity in Metals, Univ. Chicago Press, Chicago, IL, 1948, p. 158.

14. J.P. Hirth, Met. Trans. 3 (1972) 3047.

15. H.G.F. Wilsdorf, Structure and Properties of Thin Films, Wiley and Sons, New York, NY, 1959, p. 151.

16. R. M. Douthwaite and G. T. Evans, Acta Metall. 21 (1973), 525.

17. K.J. Kurzydlowski, R.A. Varin and W. Zielinski, Acta Metall. 32 (1984) 71.

18. K. Kurzydlowski, Z. Celinski and M.W. Grabski, Res Mechanica 1 (1980) 283.

19. B. Ralph, R.C. Ecob, A.J. Porter, C.Y. Barlow and N.R. Ecob, Deformation of Polycrystals: Mechanisms and Microstructure, Riso Ntl. Lab., Roskilde, Denmark, 1981, p. 111.

20. P.G. Partridge, Metall. Rev. #118 (1967).

21. W. Truszkowski, A. Latkowski and A. Dziadon, Deformation of Polycrystals: Mechanisms and Microstructure, Riso Natl. Lab., Roskilde, Denmark, 1981, p. 383.

22. M. F. Amateau, W.D. Hanna and E.G. Kendall, AF Rep. SAMSO TR-71-268 (1971).

23. F.D. Rosi, C.A. Dube and B.H. Alexander, Trans, AIME 197 (1953) 257.

24. F.D. Rosi, Trans AIME 200 (1954) 58.

25. R.N. Gardner, T.C. Pollock and H.G.F. Wilsdorf, Mater. Sci. Eng. 29 (1977) 169.

26. T.C. Pollock, Ph.D. Dissertation, U. Virginia, Charlottesville, VA 1977.

27. R.N. Gardner and H.G.F. Wilsdorf, Metall. Trans. A, 11 (1980) 653.

28. R.N. Gardner and H.G.F. Wilsdorf, Metall. Trans A, 11 (1980) 659.

29. H.G.F. Wilsdorf, Mater. Sci. Eng. 59 (1983) 1.

30. H.G.F. Wilsdorf, ZS. Metallkd. 75 (1984) 154.

DISTRIBUTION LIST

Copy No.	
1	Office of Naval Research 800 North Quincy Street Arlington, VA 22217-5000 Attention: Leader Materials Division, N00014 Associate Director for Engineering Sciences
2 - 7	Director Naval Research Laboratory Attention: Code 2627 Washington, DC 20375
8	Office of Naval Research Resident Representative, N66002 Joseph Henry Building, Room 623 2100 Pennsylvania Avenue, N.W. Washington, DC 20037
9 - 20	Defense Technical Information Center Building 5, Cameron Station Alexandria, VA 22314
21 - 22	H. G. F. Wilsdorf
23 - 24	Marjorie A. Erickson David W. Taylor Naval Ship R&D Center Annapolis Laboratory Annapolis, Maryland 21402-5067
25	K. R. Lawless Chairman, Materials Science
26 - 27	E. H. Pancake Clark Hall
28	SEAS Publications Files

JO#6673:pms

UNIVERSITY OF VIRGINIA
School of Engineering and Applied Science

The University of Virginia's School of Engineering and Applied Science has an undergraduate enrollment of approximately 1,500 students with a graduate enrollment of approximately 500. There are 125 faculty members, a majority of whom conduct research in addition to teaching.

Research is a vital part of the educational program and interests parallel academic specialties. These range from the classical engineering disciplines of Chemical, Civil, Electrical, and Mechanical and Aerospace to newer, more specialized fields of Biomedical Engineering, Systems Engineering, Materials Science, Nuclear Engineering and Engineering Physics, Applied Mathematics and Computer Science. Within these disciplines there are well equipped laboratories for conducting highly specialized research. All departments offer the doctorate; Biomedical and Materials Science grant only graduate degrees. In addition, courses in the humanities are offered within the School.

The University of Virginia (which includes approximately 1,500 full-time faculty and a total full-time student enrollment of about 16,000), also offers professional degrees under the schools of Architecture, Law, Medicine, Nursing, Commerce, Business Administration, and Education. In addition, the College of Arts and Sciences houses departments of Mathematics, Physics, Chemistry and others relevant to the engineering research program. The School of Engineering and Applied Science is an integral part of this University community which provides opportunities for interdisciplinary work in pursuit of the basic goals of education, research, and public service.

END

FILMED

1-86

DTIC